EPJ Web of Conferences **71**, 00145 (2014)
DOI: 10.1051/epjconf/20147100145

Search for the Standard Model Higgs boson in $H \longrightarrow \tau^+\tau^-$ decays in proton-proton collisions with the ATLAS detector

Zinonos Zinonas[1,a]

[1] *Georg-August-Universität Göttingen,*
II. Physikalisches Institut,
Friedrich-Hund-Platz 1 37077 Göttingen, Deutschland

Abstract. A search for the Standard Model (SM) Higgs boson decaying into a pair of τ leptons is reported. The analysis, exploiting each of the lepton-lepton, lepton-hadron and hadron-hadron di-tau final states, is based on data samples of proton-proton (pp) collisions collected by the ATLAS experiment at the Large Hadron Collider (LHC) and corresponding to integrated luminosities of 4.6 fb^{-1} and 13.0 fb^{-1} at center-of-mass energies of $\sqrt{s}$ = 7 TeV and 8 TeV, respectively. The observed (expected) upper limit at 95% CL on the cross-section times the branching ratio for SM $H \longrightarrow \tau^+\tau^-$ is found to be 1.9 (1.2) times the SM prediction for a Higgs boson with mass m_H = 125 GeV. For this mass, the observed (expected) deviation from the background-only hypothesis corresponds to a local significance of 1.1 (1.7) standard deviations.

1 Introduction

The observation of a new particle with a mass of about 125 GeV by the ATLAS and CMS experiments [1, 2] in the search for the SM Higgs boson [3, 4] is a great success of the LHC physics program and the beginning of a new era in particle physics. For a Higgs boson with a mass of 125 GeV, the $H \longrightarrow \tau^-\tau^+$ channel, with a branching ratio of 6.3% [5] is one of the leading decay modes that may provide a measurement of the coupling of the Higgs to fermions and test an important prediction of the SM.

The process with the largest SM Higgs-boson production cross-section at the LHC is gluon fusion, $gg \longrightarrow H$, with a cross-section of 15.3 pb (19.5 pb) at $\sqrt{s}$ = 7(8) TeV for m_H = 125 GeV [5], Higgs-boson production via W or Z vector-boson fusion $q'q \longrightarrow q'qH$ (denoted VBF, with cross-sections of 1.22 and 1.57 pb at $\sqrt{s}$ = 7 and 8 TeV, respectively) and via Higgs-strahlung $qq \longrightarrow VH$ (denoted VH), in association with a hadronically decaying vector boson ($V = W$ or Z), are highly relevant as well. This is due to the resulting additional jets in the final state, which provide distinct experimental signatures. In particular, the VBF topology of two high-energy jets with a large rapidity separation offers a good discrimination against background processes. For each of the aforementioned production processes, one can exploit the boost of the Higgs boson in the transverse plane by requiring additional jets of high transverse momentum (p_T) in the event. Typically, such boosted topologies exhibit larger p_T of the τ decay products and thus facilitate the measurement of the Higgs resonance signal and the discrimination of the signal from background processes.

[a] e-mail: zinonas.zinonos@phys.uni-goettingen.de

2 Analysis Strategy

Searches for the SM Higgs boson in the lepton-lepton, lepton-hadron and hadron-hadron di-tau final states are being pursued. This analysis uses pp collision data collected by the ATLAS experiment corresponding to integrated luminosities of 4.6 fb^{-1} at $\sqrt{s}$ = 7 TeV for data taken in 2011 and 13.0 fb^{-1} at $\sqrt{s}$ = 8 TeV for data recorded during 2012 between April and September [6]. The event selection used in this analysis has been optimized significantly compared to the one applied in the published ATLAS search that used 2011 data only [7]. In order to enhance the sensitivity of the search, the selected events are analyzed in several separate categories according to the number and kinematic properties of reconstructed jets. The search results using the shape of the reconstructed di-tau mass distribution from these various categories and two different data-taking periods are statistically combined according to production mode and finally for all categories. A profile likelihood ratio is used to extract measurements of the signal strength parameters, μ_{ggF} and $\mu_{\mathrm{VBF+VH}}$, defined as the ratios of measured and SM production cross-sections for the $gg \longrightarrow H$ and VBF+VH processes.

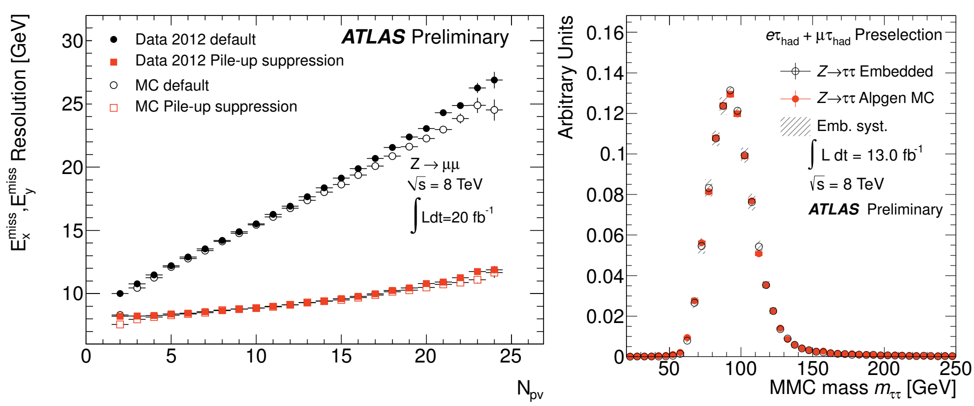

(a) E_T^{miss} resolution.

(b) MMC resolution.

Figure 1: **Left:** Resolution of the x and y E_T^{miss} components in ATLAS, as a function of the number of primary vertices for data and Monte Carlo simulation (MC) in $Z \longrightarrow \mu^+\mu^-$ candidate events. The resolution after pile-up suppression, based on the ratio of the sum p_T of the tracks associated to the primary vertex and all tracks, is also shown . **Right:** MMC di-tau mass distributions for the τ-embedded $Z \longrightarrow \mu^+\mu^-$ data and simulated $Z \longrightarrow \tau^+\tau^-$ events in the lepton-hadron channel.

3 Missing Transverse Energy

The reconstruction of the missing transverse energy, E_T^{miss} [8], uses calorimeter cells grouped into three-dimensional noise-suppressed clusters, calibrated according to the reconstructed and identified electrons, photons, hadronically decaying τ-leptons (τ_h), and jets to which they are associated. The calorimeter information of cells associated to identified muons, is replaced by the muon p_T measured by the inner detector. Cells not associated with any such objects are also taken into account in the E_T^{miss} calculation. To mitigate the impact of pile-up (PU) on E_T^{miss} in the 8 TeV data, a PU suppression technique is being pursued based on the ratio of the sum of the p_T of the tracks associated to the primary vertex (P) and the sum of the p_T of all the tracks in the event. The pile-up corrected E_T^{miss} resolution, for an average of reconstructed vertices to be around 20 in 2012, is twice smaller than the uncorrected one.

Figure 1a shows the resolution of the E_T^{miss} in 2012, as a function of the number of reconstructed primary vertices in the event.

4 Di-tau mass reconstruction

The tau-pair invariant mass is the final discriminating observable used for this analysis. The di-tau mass is reconstructed by means of the Missing Mass Calculator (MMC) [9], except for 7 TeV data in the lepton-lepton channel. This technique provides a reconstruction of event kinematics in the di-tau final state with high efficiency (> 99%) and reasonable mass resolution (13 − 20%), depending on the event topology and final state; better resolution is obtained for events with boosted Higgs and in final states with fewer neutrinos. Conceptually, the MMC is a more sophisticated version of the simple collinear approximation [10]. The latter method has the disadvantage of providing unphysical solutions for about 1/5 of the events, in particular when the E_T^{miss} and the parent boson p_T are relatively small. The main improvement in MMC comes from requiring that relative orientations of the neutrinos and other decay products are consistent with the mass and kinematics of a τ lepton decay. This is achieved by maximizing a probability defined in the kinematically allowed phase space region. In the lepton-lepton analysis at 7 TeV, the collinear approximation was used to reconstruct the mass of the di-tau system in all categories with at least one jet. For lepton-lepton events with no jets, the invariant mass of the di-lepton and E_T^{miss} system, referred to as effective mass $m_{\tau\tau}^{\text{eff}}$, was used because the performance of the collinear approximation is not optimal in events where the τ-decay products are back-to-back in the transverse plane. A typical distributions of the reconstructed $m_{\tau\tau}$ in $Z \longrightarrow \tau^+\tau^-$ events is shown in Figure 1b.

5 Event Categorization

Even after the application of topological selections, it is still not possible to extract any meaningful signal from the inclusive di-tau invariant mass distribution, due to the very low signal purity. In order to increase the signal over background ratio, events have been categorized in terms of the number of jets with p_T above a given threshold, depending also on the the final state considered:

- 0-jet event category: very similar to the inclusive category. It is used to constraint the experimental uncertainties, rather fitting any signal.
- 1-jet event category: depending on a selection applied on events with at least 1 jet and the final state, the category is further divided into the VH and Boosted Higgs category;
  - VH category
  - Boosted Higgs category
- 2-jet category: this category is designed to mostly select events from VBF and VH production mechanism. Some contribution from gluon fusion is inevitable due to its high cross-section;
  - VH category
  - VBF category: the selection cuts of the VBF jets are similar but not identical. Two jets with p_T above 30 GeV must be present, with quite large invariant mass. A selection on the difference in pseudo-rapidity of the two jets is also required, as well as the veto on any jet activity between the two.

Different categories are applied in different final states. For example, in the hadron-hadron final state only the VBF and the Boosted Higgs categories are used.

6 Background estimation

The largest source of background is the Drell-Yan production of $Z \longrightarrow \tau^+\tau^-$, which is modeled using an embedding procedure. In a sample of selected $Z \longrightarrow \mu^+\mu^-$ data events, the muon tracks and associated calorimeter cells are replaced by τ leptons from a simulated $Z \longrightarrow \tau^+\tau^-$ decay with the same kinematics. These simulated τ decays are then merged with the initial data event. Therefore, only the τ decays and the corresponding detector response are taken from the simulation, whereas jets, underlying event (UE) and all other event properties including PU effects are obtained directly from the data. Modeling of the major background by means of embedded $Z \longrightarrow \tau^+\tau^-$, events has the following advantage: a data-driven description of the entire event, except for τ-lepton decays, leading to significantly reduced systematic uncertainties compared to what can be achieved with the fully simulated samples [6].

The Drell-Yan production of $Z \longrightarrow \ell\ell$, where ℓ denotes the e or μ lepton, is an important source of background in the lepton-lepton and lepton-hadron channel, due to the fact that the reconstructed $m_{\tau\tau}$ distribution peaks in the Higgs boson mass search range. In particular, this background source is important for the electron-hadron had final state owing to the non-negligible probability for electrons to be misidentified as hadronic taus. The contribution of this background in the lepton-hadron channels is estimated by MC simulation using correction factors obtained by comparing simulation to data.

The fake lepton background consists of events that have a reconstructed lepton that did not originate from the decay of a τ lepton or the leptonic decay of a W or Z boson. The normalization and shape of relevant distributions are obtained from data with control regions in which the lepton isolation requirement is reversed. The background from W + jets production contributes significantly to the electron- and muon-hadron channels when the W decays leptonically and one jet is misidentified as a hadronic tau. The background is modeled for these channels using simulated samples but the yield is normalized to data using control regions requiring a high cut on the transverse mass, $m_T = \sqrt{2\, p_T^\ell\, E_T^{\rm miss} \left(1 - \cos\phi_{\ell, E_T^{\rm miss}}\right)}$. Figure 2b shows the predicted and observed m_T distribution obtained in the muon-hadron channel at the preselection stage of the analysis.

QCD multi-jet events, in which one jet is misidentified as a hadronic τ and another as a lepton (e or μ), constitute another important source of background in the lepton-hadron channel. The background estimation is entirely based on observed data using control samples where the lepton and the hadronic taus are required to have the same electric charge (SS). The expected contribution of the QCD multi-jet background is then rescaled by corrections derived from a QCD multi-jet enriched region in data, that account for potential differences in jet $\rightarrow \ell$ and jet $\rightarrow$ hadronic tau fake rates introduced by the same or opposite sign charge requirements.

The large QCD multi-jet production is also one of the dominant backgrounds in the hadron-hadron channel and data-driven methods are used to estimate its shape and normalization. The QCD multi-jet mass shape is extracted from data samples with minimal true-τ contamination. In the 7 TeV dataset, the shape is obtained from data events in which all kinematic criteria are the same as those used to define the signal region, but the two hadronic tau candidates do not have opposite charge (anti-opposite sign – notOS). In the 8 TeV dataset, the QCD multi-jet shape comes from OS data events in which the tau identification criteria have been reversed compared to the signal region. This procedure has a clear advantage in modeling the low-mass tail of the $m_{\tau\tau}$ distribution. The QCD multi-jet normalization is obtained by performing a two-dimensional template fit to the track multiplicity distributions of the two hadronic tau candidates. The tracks associated to the tau candidates are counted in the cone

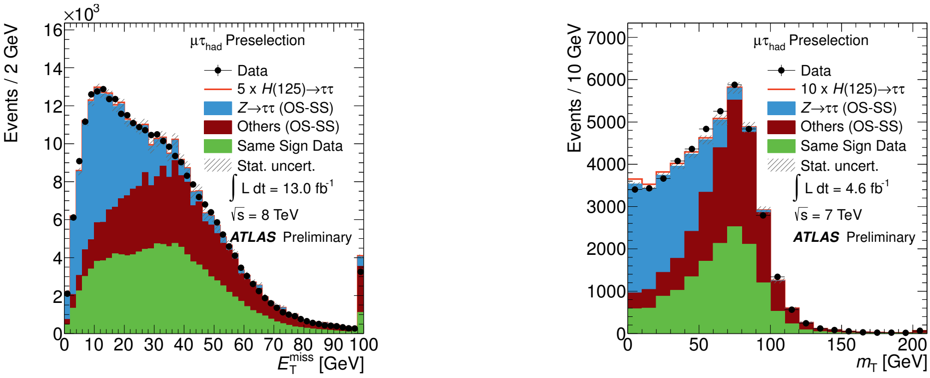

(a) E_T^{miss} distribution.

(b) m_T distribution.

Figure 2: **Left:** Missing transverse energy distribution in the muon-hadron channel at preselection. **Right:** Transverse mass distribution in the muon-hadron channel after applying preselection cuts.

defined by $\Delta R < 0.6$. The contribution from di-tau events is a free parameter in the fit. The multi-jet template is modeled from a sample of SS candidates in the data. The $W \longrightarrow \tau\nu$ + jets accounts for a non-negligible source of background events in the hadron-hadron channel. In such events, a jet is usually misidentified as a hadronic tau candidate. This type of background events is estimated by simulation.

The predicted yield of the $t\bar{t}$ background process for all channels is obtained from simulation, with the yield rescaled to the one observed using a $t\bar{t}$-enriched control sample, extracted by requiring b-tagged jets.

Finally, the small background contribution in each channel from di-boson and single-top production is estimated using the simulation.

7 Evaluation of the systematics uncertainties

In order to parametrize the signal and background uncertainties, several nuisance parameters are introduced in the fit to the mass shape. These nuisances can represent either the uncertainty on the total normalization of a background or describe the uncertainty in the shape of the distribution. Theoretical uncertainties on the signal cross section are considered as well. The fit itself, through the background sidebands, can constraint these parameters and in some cases the uncertainty is greatly reduced with respect to what used in input. The most important systematics are those affecting the background normalization like the tau identification (ID) efficiency or the migration from one category to another due to the jet energy scale. Other kind of uncertainties are those related to the mass shape like the tau and E_T^{miss} energy scale. When the number of events in the samples used to extract the mass shape is limited, bin-by-bin uncertainties are used, i.e. each bin in the template is let fluctuate independently from any other. This is the most conservative shape uncertainties to be applied.

Table 1 shows how some of the uncertainties affect the normalization of the backgrounds and signal samples. The ranges reflect the effect in the various categories and final states.

Table 1: Summary of $Z \longrightarrow \tau^+\tau^-$ background and signal systematic uncertainties by channel (percentage numbers). The quoted ranges refer specifically to the 8 TeV dataset, but they are similar for the 7 TeV dataset. Uncertainties indicated with (S) are also applied bin-by-bin, and therefore affect the shape of the final distributions. Signal systematic uncertainties are derived from the sum of all signal production modes.

Uncertainty	lepton-lepton	lepton-hadron	hadron-hadron
		$Z \longrightarrow \tau\tau$	
Embedding	1-4 (S)	2-4 (S)	1-4 (S)
Tau energy scale	-	4-15 (S)	3-8 (S)
Tau identification	-	4-5	1-2
Trigger efficiency	2-4	2-5	2-4
Normalization	5	4 (non-VBF), 16 (VBF)	9-10
		Signal	
Embedding	1-5 (S)	3-9 (S)	2-4 (S)
Tau energy scale	-	2-9 (S)	4-6 (S)
Tau identification	-	4-5	10
Trigger efficiency	small	small	5
Theory	8-28	18-23	3-20

8 Statistical analysis

The profile likelihood formalism is used in this statistical analysis incorporating the information on the observed and expected number of events, nuisance parameters, probability density functions and parameters of interest. The statistical significance of an excess is evaluated in terms of the same profile likelihood test statistic. The observed 95% Confidence Level (CL) upper limit is obtained using the modified frequentist construction CLs [11, 12]. The expected hypothesis is quantified using the p-value, the probability that the test statistic of a background-only experiment fluctuates to at least the observed value sensitivity and the ± 1, 2 σ bands are obtained for the background expectation in the absence of a SM Higgs boson signal. The consistency with the background-only hypothesis is quantified using the p-value, the probability that the test statistic of a background-only experiment fluctuates to at least the observed value.

9 Results

The most sensitive categories are the Boosted, 2-jet VBF and 1-jet categories in the lepton-hadron channel, and the 2-jet VBF category for both the hadronic channels. Distributions for the final discriminating variable $m_{\tau\tau}$ are shown in Figures 3a-3f. No significant excess is observed in the data compared to the SM background-only expectation in any of the channels studied.

Figure 4a shows expected and observed cross-section limits for the combination of all three channels for 2011 and 2012 data as a function of the Higgs boson mass at the 95% CL. The combined expected limit varies between 1.2 and 3.4 times the predicted SM cross-section times branching ratio for the mass range between 100 and 150 GeV. The corresponding observed limits are in the range between 1.9 and 3.3 times the predicted SM cross-section times branching ratio for the same mass range. For $m_H = 125$ GeV specifically, the expected limit is 1.2 and the observed 1.9.

Figure 4b shows the observed and expected p_0 values as a function of the Higgs boson mass corresponding to SM Higgs boson signal introduced with signal strength $\mu = 1$ at the mass in question.

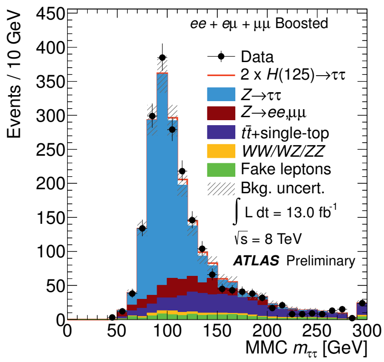

(a) Lepton-lepton Boosted category

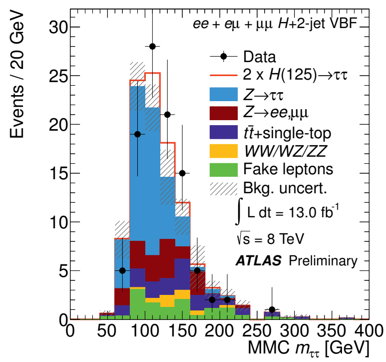

(b) Lepton-lepton VBF category

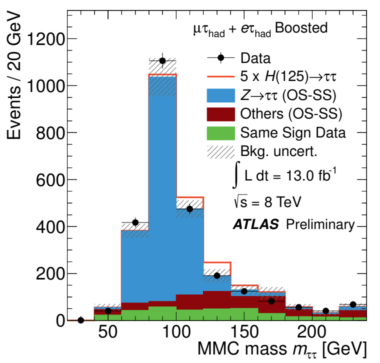

(c) Lepton-hadron Boosted category

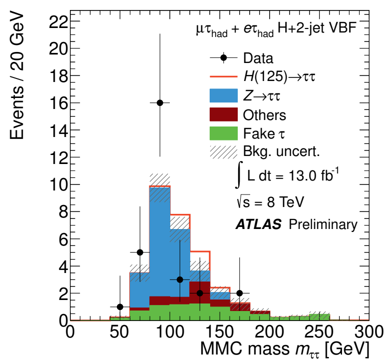

(d) Lepton-hadron VBF category

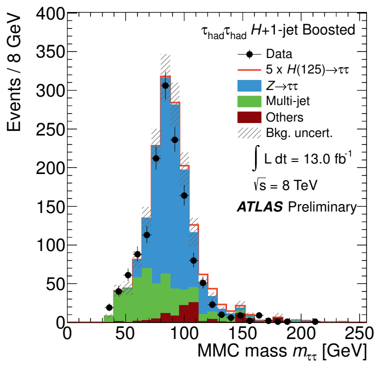

(e) Hadron-hadron Boosted category

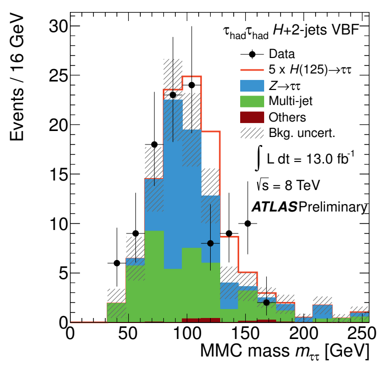

(f) Hadron-hadron VBF category

Figure 3: Reconstructed $m_{\tau\tau}$ distributions for the 2-jet VBF and 1-jet Boosted categories at $\sqrt{s}$ = 8 TeV.

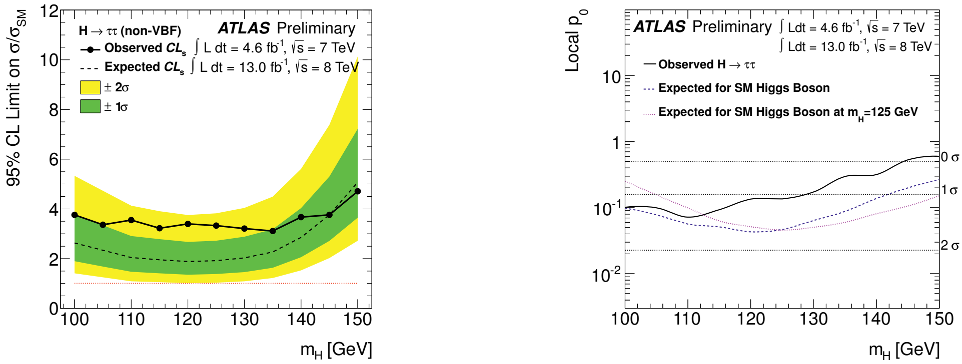

(a) 95% CL upper limits

(b) p_0-value

Figure 4: **Left:** Combined observed 95% CL upper limit on the signal strength parameter $\hat{\mu} = \sigma/\sigma_{\rm SM}$, together with the expected limit obtained in the background hypothesis, as a function of the Higgs boson mass, m_H. The bands show the expected one- and two-standard-deviation probability intervals around the expected limit. **Right:** The solid and dashed lines describe observed and expected p_0 values, respectively, as a function of the Higgs boson mass corresponding to SM Higgs boson signal introduced with signal strength $\hat{\mu} = 1$ at the mass in question. The dotted line shows the expected p_0 calculated for the case when a SM Higgs boson signal at $m_H = 125$ GeV is tested as a function of the Higgs boson mass.

The dotted line shows the expected p_0 calculated for the case when a SM Higgs boson signal at $m_H = 125$ GeV is tested as a function of the Higgs boson mass. The most significant deviation from the background-only hypothesis is observed for $m_H = 110$ GeV with a local p-value of 7.2%.

10 Conclusions

A search for a SM Higgs boson decaying in the $H \longrightarrow \tau^+\tau^-$ channel has been performed with the ATLAS detector at the LHC [6]. The lepton-lepton, lepton-hadron and hadron-hadron di-tau decays are considered in this search, which uses the full 2011 data sample collected at a center-of-mass energy of 7 TeV and 13.0 fb^{-1} of 8 TeV data collected in 2012. The observed (expected) upper limit at 95% CL on the cross-section times branching ratio for SM $H \longrightarrow \tau^+\tau^-$ is found to be 1.9 (1.2) times the SM prediction for a Higgs boson with mass $m_H = 125$ GeV. For this mass, the observed (expected) deviation from the background-only hypothesis corresponds to a local significance of 1.1 (1.7) standard deviations and the best fit value of $\mu = 0.7 \pm 0.7$.

References

[1] G. Aad et al. [ATLAS Collaboration], “Observation of a new particle in the search for the Standard Model Higgs boson with the ATLAS detector at the LHC”, Phys. Lett. B 716, 1 (2012) [arXiv:1207.7214 [hep-ex]].

[2] S. Chatrchyan et al. [CMS Collaboration], “Observation of a new boson at a mass of 125 GeV with the CMS experiment at the LHC”, Phys. Lett. B 716, 30 (2012) [arXiv:1207.7235 [hep-ex]].

[3] F. Englert and R. Brout, “Broken symmetries and the masses of gauge bosons”, Phys. Rev. Lett. 321, 13 (1964).

[4] Higgs, P. W., “Broken symmetries and the masses of gauge bosons”, Phys. Rev. Lett., 508, 13 (1964).

[5] S. Dittmaier et al. (LHC Higgs Cross Section Working Group), arXiv:1101.0593 [hep-ph].

[6] “Search for the Standard Model Higgs boson in H-> tau tau decays in proton-proton collisions with the ATLAS detector”, ATLAS-CONF-2012-160, Nov 2012.

[7] ATLAS Collaboration, JHEP 1209 (2012) 70, arXiv:1206.5971 [hep-ex].

[8] G. Aad et al. [ATLAS Collaboration], “Performance of Missing Transverse Momentum Reconstruction in Proton-Proton Collisions at 7 TeV with ATLAS”, Eur. Phys. J. C 72, 1844 (2012) [arXiv:1108.5602 [hep-ex]], https://twiki.cern.ch/twiki/bin/view/AtlasPublic/JetEtmissApproved2013EtMiss .

[9] A. Elagin, P. Murat, A. Pranko and A. Safonov, “A New Mass Reconstruction Technique for Resonances Decaying to di-tau”, Nucl. Instrum. Meth. A 654, 481 (2011) [arXiv:1012.4686 [hep-ex]].

[10] R. K. Ellis, I. Hinchliffe, M. Soldate and J. J. van der Bij, “Higgs Decay to $\tau^+\tau^-$: A Possible Signature of Intermediate Mass Higgs Bosons at the SSC,” Nucl. Phys. B 297, 221 (1988).

[11] A. L. Read, ”Presentation of search results: The CL(s) technique“, J. Phys. G 28, 2693 (2002).

[12] ATLAS Collaboration, ”Procedure for the LHC Higgs boson search combination in summer 2011“, ATL-PHYS-PUB-2011-011, CERN, Geneva, Aug 2011